ELSEVIER

Journal of Organometallic Chemistry 536–537 (1997) 93–107

Journal of Organometallic Chemistry

Preparation and thermolysis of complexes derived from some trinuclear ruthenium clusters and 1,4-diphenylbuta-1,3-diyne [1]

Michael I. Bruce [a,*], Natasha N. Zaitseva [a], Brian W. Skelton [b], Allan H. White [b]

[a] *Department of Chemistry, University of Adelaide, Adelaide, S.A. 5005, Australia*
[b] *Department of Chemistry, University of Western Australia, Nedlands, W.A. 6907, Australia*

Received 25 April 1996; accepted 9 May 1996

Abstract

Reactions between $Ru_3(\mu\text{-dppm})(CO)_{10}$ and PhC≡CC≡CPh in thf, in the presence of Me_3NO, afford the complexes $Ru_3(\mu_3\text{-}PhC_2C{\equiv}CPh)(\mu\text{-dppm})(\mu\text{-CO})(CO)_7$ (**1**) and $Ru_3(\mu\text{-dppm})\{\mu\text{-}C_4Ph_2(C{\equiv}CPh)_2\}(CO)_6$ (**2**). Complex **1** was also obtained from $Ru_3(\mu_3\text{-}PhC_2C{\equiv}CPh)(\mu\text{-CO})(CO)_9$ (**3**) and dppm in thf on heating. Two of the complexes formed by thermolysis of **1** in xylene at 130 °C were identified crystallographically as $Ru_3\{\mu_3\text{-}CPhCHCC(C_6H_4\text{-}2)\}(\mu\text{-dppm})(CO)_8$ (**4**) and $Ru_3\{\mu_3\text{-}C_4H_2Ph_2\}(\mu\text{-CO})(CO)_5(dppm)$ (**5**). In **4**, fragmentation of the cluster and metallation of one of the diyne phenyl groups took place; the dppm ligand bridges two non-bonded Ru atoms. In **5**, partial hydrogenation of the diyne has occurred to give a $2\eta^1{:}\eta^4{:}\eta^4$-butadiendiyl ligand, the dppm ligand adopting a chelating mode on one of the two Ru atoms which is η^4 attached to the hydrocarbon. In comparison, thermolysis of **3** gave $Ru_4(\mu_4\text{-}PhC_2C{\equiv}CPh)(CO)_n$ (n = 12 (**6**) and 14 (**7**)). The former has a distorted C_2Ru_4 octahedral core, while in the latter the Ru_3 cluster has fragmented to give a ruthenacyclopentadiene derivative in which the central C–C bond bridges an $Ru_2(CO)_8$ group.
© 1997 Elsevier Science S.A.

Keywords: Ruthenium; Carbonyl; Diyne complexes; Clusters; Crystal structure

1. Introduction

We have recently described reactions between $Ru_3(CO)_{12}$ or its 'activated' derivative, $Ru_3(CO)_{10}(NCMe)_2$, with 1,4-diphenylbuta-1,3-diyne to give several complexes which are similar in structural type to other complexes obtained from alkynes and these carbonyl precursors [1]. Other groups have studied the chemistry of several ruthenium and osmium cluster carbonyls with 1,3-diynes [2–4], and this work was summarised in our earlier paper. We have also reported the synthesis of a bow-tie Ru_3Co_2 complex retaining the diyne ligand from the reaction between $Ru_3(\mu_3\text{-}PhC_2C{\equiv}CPh)(\mu\text{-CO})(CO)_9$ and $Co_2(CO)_8$, probably by attack of the Co reagent on the Ru_3 framework [5], and of a related complex in which the central C–C bond of the diyne has been cleaved, which was obtained from $Co_2(CO)_8$ and $Ru_3(\mu_3\text{-}PhC_2C{\equiv}CPh)(\mu\text{-dppm})(\mu\text{-CO})(CO)_7$ (**1**) [6]. In contrast, the reaction between the Os_3 carbonyl analogue and $Co_2(CO)_8$ results in the formation of $\{Co_2(CO)_6\}_2(\mu,\mu\text{-}PhC_2C_2Ph)$, while addition of a $Co_2(CO)_6$ fragment to the free C≡C triple bond of the complex $Os_3\{\mu_3\text{-}HC_2C{\equiv}CSiMe_3\}(\mu\text{-CO})(CO)_9$ is found in that case [7]. In general, the chemistry of $Ru_3(\mu\text{-dppm})(CO)_{10}$ gives cleaner reactions than does $Ru_3(CO)_{12}$, and this was also found to be true for its reaction with PhC≡CC≡CPh, from which complex **1** was obtained. This paper describes this reaction in detail, together with a study of the thermolysis behaviour of **1** and of the related unsubstituted complex $Ru_3(\mu_3\text{-}PhC_2C{\equiv}CPh)(\mu\text{-CO})(CO)_9$.

2. Results

The reaction between $Ru_3(\mu\text{-dppm})(CO)_{10}$ and PhC≡CC≡CPh was carried out in thf in the presence of Me_3NO at room temperature overnight. Purification of the reaction mixture was accomplished by thin-layer chromatography (t.l.c.), which separated unreacted $Ru_3(\mu\text{-dppm})(CO)_{10}$ (42%) from dark red crystalline $Ru_3(\mu_3\text{-}PhC_2C{\equiv}CPh)(\mu\text{-dppm})(\mu\text{-CO})(CO)_7$ (**1**;

* Corresponding author.

[1] Dedicated to the memory of Yuri T. Struchkov, outstanding crystallographer, colleague and friend.

0022-328X/97/$17.00 © 1997 Elsevier Science S.A. All rights reserved.
PII S0022-328X(96)06492-3

Scheme 1) (36%) and dark purple $Ru_3(CO)_6(dppm)(PhC_4Ph)_2$ (**2**) (7%). Complex **1** was also obtained in 66% yield from a reaction between $Ru_3(\mu_3\text{-}PhC_2C{\equiv}CPh)(\mu\text{-}CO)(CO)_9$ (**3**) and dppm in refluxing thf for 10 min.

The identification of **1** as a simple substitution product of the alkyne cluster was indicated by its IR ν(CO) spectrum, which was similar to those of other complexes $Ru_3(\mu_3\text{-alkyne})(\mu\text{-dppm})(\mu\text{-CO})(CO)_7$ which have been described on previous occasions [8,9]. The ^{1}H NMR spectrum was uninformative, containing only resonances from the Ph groups between δ 6.92 and 7.51 and the two CH_2 protons of the dppm ligand at δ 4.49 and 5.81. The FAB mass spectrum contained M^+ centred on m/z 1115 and fragment ions formed by loss of up to seven CO and two Ph groups. The molecular structure was confirmed by the single crystal X-ray study described below.

Complex **2** could not be obtained in crystalline form suitable for X-ray studies. The formula was established by elemental analysis and from the FAB mass spectrum, which contained M^+ centred at m/z 1261 and ions formed by stepwise loss of up to six CO groups and two Ph groups. The ^{1}H NMR spectrum was uninformative. However, when the original reaction was carried out using an excess of PhC≡CC≡CPh, or when **1** is treated with one equivalent of diyne, a fast reaction ensues

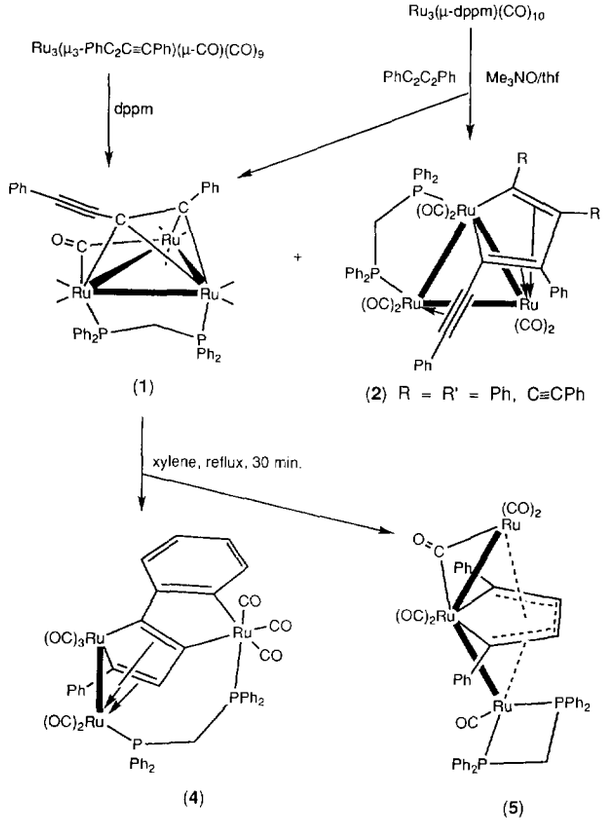

Scheme 1.

which converts **1** to **2** in up to 50% yield. In attempts to obtain crystals of complexes related to **2**, reactions of **1** with a variety of alkynes were examined. Although rapid reactions to give analogous products occurred, none gave X-ray quality crystals. Only with $Me_3SiC{\equiv}CC{\equiv}CSiMe_3$ were crystalline products obtained. However, none of these appeared to be similar in composition to **2** (as indicated, for example, by their IR ν(CO) spectra) and the variety of structural types obtained in these experiments will be described elsewhere.

Complex **1** is quite stable, only decomposing in refluxing xylene after 30 min. Although several complexes were formed in this reaction, only two were obtained in crystalline form. The major product was a bright yellow solid shown to be an isomer of **1** by a single crystal X-ray study (below) with the formula $Ru_3\{\mu_3\text{-}CPhCHCC(C_6H_4\text{-}2)\}(\mu\text{-dppm})(CO)_8$ (**4**; Scheme 1). The IR ν(CO) spectrum contained seven bands between 2088 and 1923 cm^{-1} and the ^{1}H NMR spectrum three multiplets for the aromatic protons between δ 6.68 and 7.76, together with a well-resolved quartet for one of the CH_2 protons at δ 2.23. The remaining signal in the spectrum, at δ 1.37, appears to be a superposition of two resonances, from the second CH_2 proton and from the single ring proton. The relatively large upfield shift of these resonances, compared with those found in the precursor, may reflect the non-chelate character of the ligand, which has the relatively large P(1)–C(0)–P(2) angle of 124.0(2)° (see below). The FAB mass spectrum contains a molecular ion centred on m/z 1115 which shows loss of eight CO ligands and two Ph groups.

An orange band afforded red crystals, shown to have the structure $Ru_3(\mu_3\text{-}C_4H_2Ph_2)(\mu\text{-CO})(CO)_5(dppm)$ (**5**) by an X-ray study (below). The IR ν(CO) spectrum contains only three medium to strong absorptions in the terminal region, together with a weak band assigned to the μ-CO ligand at 1808 cm^{-1}. In the ^{1}H NMR spectrum, a multiplet at δ 0.91 is assigned to the ring protons, two signals at δ 4.21 and 4.95 to the two CH_2 protons, and a multiplet between δ 6.50 and 7.49 to the aromatic protons. The M^+ ion is found centred on m/z 1061 in the FAB mass spectrum, which also contains ions formed by loss of three and four CO groups, together with the unusual fragment ions $[M - Ru - nCO]^+$ (n = 5 and 6).

2.1. Thermolysis of $Ru_3(\mu_3\text{-}PhC_2C{\equiv}CPh)(\mu\text{-CO})(CO)_9$

It was of interest to compare the thermolysis of **1** with that of the unsubstituted complex **3**, the preparation and structure of which have been described on previous occasions [1,10]. Thermolysis of **3** in xylene at 120 °C (oil-bath temperature) over a period of 30 min, followed by separation of the products by preparative

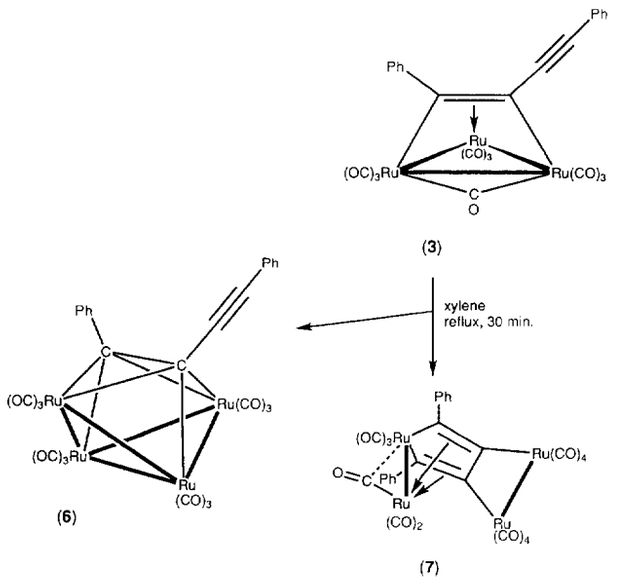

Scheme 2.

t.l.c., resulted in the isolation of two tetranuclear complexes (Scheme 2). The yields were low and, under these conditions, only about 35% of the total ruthenium was recovered.

The first complex was obtained in 14% yield and readily identified as the previously described complex $Ru_4(\mu_4\text{-}PhC_2C{\equiv}CPh)(CO)_{12}$ (**6**) [1] by comparison with an authentic sample (infrared and mass spectrometry) and by a second X-ray structural determination (not reported here).

A second yellow complex was identified as $Ru_4(CO)_{14}(PhC_4Ph)$ (**7**) by mass spectrometry with M^+ at m/z 1000 and ions formed by stepwise loss of up to 14 CO groups. The infrared spectrum contained eight medium to strong intensity ν(CO) bands. Although the frequency of the highest of these (2126 cm^{-1}) suggested the presence of a free C≡C triple bond, the X-ray structural determination showed that this was not the case. A broad band at 1915 cm^{-1} is assigned to the bridging CO group found in the solid-state structure. A single-crystal X-ray structural determination established the structure of **7** as that shown in the scheme.

2.2. X-ray structural studies

2.2.1. Molecular structure of $Ru_3(\mu_3\text{-}PhC_2C{\equiv}CPh)(\mu\text{-dppm})(\mu\text{-CO})(CO)_7$ (1)

A plot of a molecule of **1** is shown in Fig. 1. Significant bond parameters are collected in Table 1. Relevant comparisons are with the structures of $Ru_3(\mu\text{-}H)_2\{\mu_3\text{-}C_2(CO_2Me)_2\}(\mu\text{-dppm})(CO)_8$ (**8**) [9] (there is no other published structure of a complex $Ru_3(\mu_3\text{-}C_2R_2)(\mu\text{-dppm})(CO)_8$) and $Ru_3(\mu_3\text{-}PhC_2C{\equiv}CPh)(\mu\text{-CO})(CO)_9$ (**3**) [10]. As can be seen, the molecule contains a triangular Ru_3 core, surmounted by the alkyne, which is attached through only one of the two C≡C triple bonds. One edge of the triangle is bridged by the dppm ligand and a second edge by a μ-CO ligand. Coordination is completed by seven terminal CO groups.

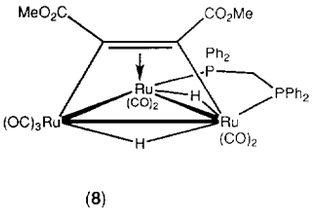

The three Ru–Ru separations are 2.711(1) Å (non-bridged, 2.715(1) in **3**), 2.794(1) Å (bridged by dppm; 2.836(1) Å in **8** (but also bridged by H); 2.834(1) in $Ru_3(\mu\text{-dppm})(CO)_{10}$ [11]) and 2.865(1) Å (bridged by CO; 2.839(1) Å in **3**). The Ru(2)–Ru(3) vector is unsymmetrically bridged by CO(23) (Ru(2,3)–C(23) 1.998(7), 2.284(8) Å, angles Ru(2,3)–C(23)–O(23) 145.9(6), 130.3(5)°; values for **3** 1.995(8), 2.469(6) Å, 127.7, 154.0(5)°) as found in similar complexes. There is a corresponding asymmetry in the attachment of the

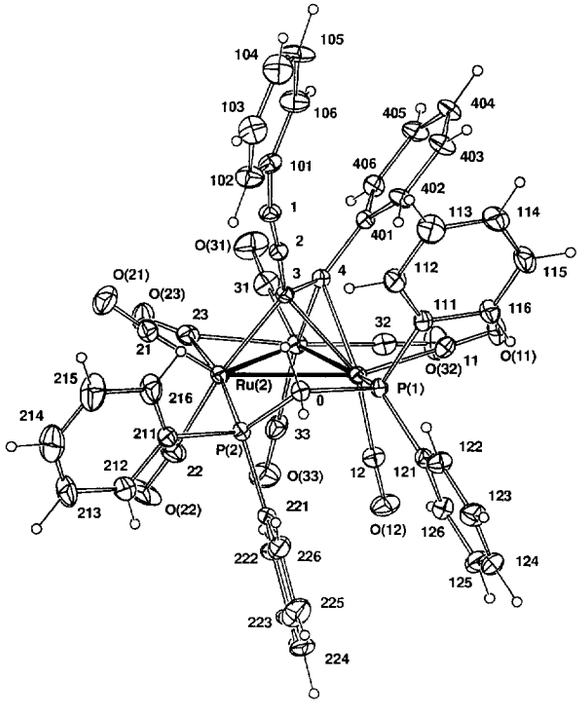

Fig. 1. Plot of a molecule of $Ru_3(\mu_3\text{-}PhC_2C \equiv CPh)(\mu\text{-dppm})(\mu\text{-CO})(CO)_7$ (**1**), showing the atom numbering scheme. In this and subsequent figures, non-hydrogen atoms are shown with 20% thermal envelopes; hydrogen atoms have arbitrary radii of 0.1 Å.

Table 1
Selected bond parameters for $Ru_3(\mu_3\text{-}PhC_2C \equiv CPh)(\mu\text{-}dppm)(\mu\text{-}CO)(CO)_7$ (**1**)

Bond lengths (Å)		Bond angles (deg)	
Ru(1)–Ru(2)	2.794(1)	Ru(1)–Ru(2)–P(2)	79.00(5)
Ru(1)–Ru(3)	2.711(1)	Ru(2)–Ru(1)–P(1)	100.99(5)
Ru(2)–Ru(3)	2.865(1)	Ru(1)–P(1)–C(0)	106.7(2)
Ru(1)–P(1)	2.337(2)	Ru(2)–P(2)–C(0)	114.5(2)
Ru(2)–P(2)	2.362(2)	P(1)–C(0)–P(2)	107.9(3)
Ru(1)–C(3)	2.243(6)		
Ru(1)–C(4)	2.250(5)	C(401)–C(4)–C(3)	123.6(6)
Ru(2)–C(3)	2.123(7)	C(4)–C(3)–C(2)	123.3(6)
Ru(3)–C(4)	2.097(7)	C(3)–C(2)–C(1)	174.6(7)
Ru(2)–C(23)	1.998(7)	C(2)–C(1)–C(101)	171.2(8)
Ru(3)–C(23)	2.284(8)		
P(1)–C(0)	1.813(7)	Ru(2)–C(23)–O(23)	145.9(6)
P(2)–C(0)	1.828(8)	Ru(3)–C(23)–O(23)	130.3(5)
C(1)–C(2)	1.20(1)		
C(2)–C(3)	1.44(1)		
C(3)–C(4)	1.383(8)		

alkyne ligand. Atoms C(3) and C(4) of the diyne are attached to all three Ru atoms, in σ-type bonds to Ru(2) and Ru(3) (2.123 Å, 2.097(7) Å respectively; cf. 2.078(5), 2.132(4) Å in **3**) and π-bonded to Ru(1) (2.243(6), 2.250(5) Å; cf. 2.205, 2.290(5) Å in **3**). A PhC≡C group is attached to C(3) (C(2)–C(3) 1.44(1), C(1)–C(2) 1.20(1) Å) and a Ph group to C(1). The substituent bend-back angles at C(3) and C(4) are 123.3(6)° and 123.6(6)° respectively (cf. 124.8(4)° and 121.1(4)° for **3**).

The geometry of the μ-dppm ligand is similar to that found in many other Ru_3 clusters bearing this ligand. The Ru–Ru–P angles at Ru(1) and Ru(2) are 100.99(6)° and 79.00(5)° respectively, which may be compared with values of 95.5(1)° and 89.4(1)° found for $Ru_3(\mu\text{-}dppm)(CO)_{10}$ [11]. Similarly, angles at the two P atoms and at the CH_2 carbon are 106.7(2), 114.5(2) and 107.9(3)°. The relatively large angle at Ru(1) is also reflected in the respective Ru(3)–Ru(*n*)–CO(11,12) (*n* = 1, 2) angles and may result from the lower effective coordination number of Ru(1) vs. Ru(2).

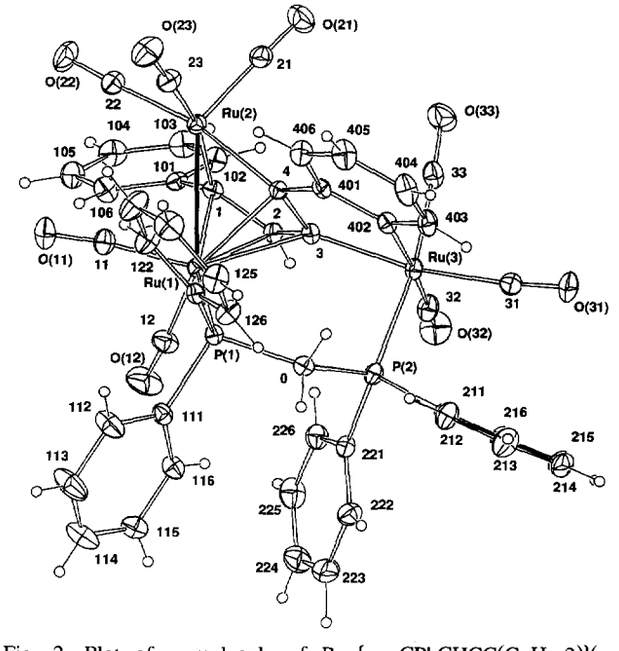

Fig. 2. Plot of a molecule of $Ru_3\{\mu_3\text{-}CPhCHCC(C_6H_4\text{-}2)\}(\mu\text{-}dppm)(CO)_8$ (**4**), showing the atom numbering scheme.

2.2.2. *Molecular structure of $Ru_3(\mu_3\text{-}CPhCHCC(C_6H_4\text{-}2)\}(\mu\text{-}dppm)(CO)_8$ (4)*

Fig. 2 is a plot of a molecule of **4**, and important bond distances and angles are given in Table 2. In this complex, only two of the Ru atoms are bonded to each other as part of an $Ru_2(\mu\text{-}C_4H_4)(CO)_6$-type structure, which can be compared with that of $Ru_2\{\mu\text{-}C(C{\equiv}CPh){=}CPhC(C{\equiv}CPh){=}CPh\}(CO)_6$ (**9**) [1]. One Ru is also attached to the dppm ligand, the second P atom of which is bonded to the third Ru atom, which is also chelated by a ring carbon and a carbon of a metallated C_6H_4 ring. Three CO ligands make up the octahedral coordination around this ruthenium.

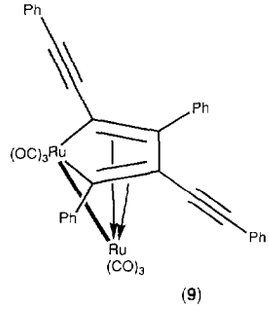

(9)

The Ru(1)–Ru(2) bond is 2.727(2) Å (cf. 2.703(3) Å

Table 2
Selected bond parameters for $Ru_3\{\mu_3\text{-}CPhCHCC(C_6H_4\text{-}2)\}(\mu\text{-}dppm)(CO)_8$ (**4**)

Bond lengths (Å)		Bond angles (deg)	
Ru(1)–Ru(2)	2.727(2)	C(1)–Ru(2)–C(4)	77.7(1)
Ru(1)–P(1)	2.329(1)	Ru(1)–P(1)–C(0)	118.4(1)
Ru(3)–P(2)	2.383(2)	Ru(3)–P(2)–C(0)	116.7(1)
Ru(1)–C(1)	2.240(3)	P(1)–C(0)–P(2)	124.0(2)
Ru(1)–C(2)	2.253(4)	C(3)–Ru(3)–C(402)	77.5(1)
Ru(1)–C(3)	2.304(4)		
Ru(1)–C(4)	2.255(5)	C(3)–Ru(3)–C(33)	80.3(2)
Ru(2)–C(1)	2.082(4)	C(33)–Ru(3)–C(402)	85.4(2)
Ru(2)–C(4)	2.107(3)	P(2)–Ru(3)–C(402)	84.8(1)
Ru(3)–C(3)	2.107(4)		
Ru(3)–C(402)	2.128(4)	Ru(2)–C(1)–C(2)	115.0(3)
P(1)–C(0)	1.843(4)	C(1)–C(2)–C(3)	117.4(3)
P(2)–C(0)	1.839(4)	C(2)–C(3)–C(4)	112.9(3)
C(1)–C(2)	1.410(5)	Ru(2)–C(4)–C(3)	115.5(3)
C(3)–C(3)	1.416(5)	Ru(3)–C(3)–C(4)	117.8(3)
C(3)–C(4)	1.436(5)		

in **9**) and, unusually, is not bridged by a CO group. This results from the almost eclipsed conformation of the CO groups on Ru(1) and Ru(2) and resembles the situation found in $Ru_2(\mu\text{-}CFc{=}CHCH{=}CFc)(CO)_6$ (Fc = ferrocenyl) [12]. With Ru(2), atoms C(1–4) form a ruthenacyclopentadiene ring, with Ru(2) σ-bonded to C(1,4) (2.082(4), 2.107(3) Å; 2.06, 2.07(2) Å in **9**) and Ru(1) attached to all four carbons (2.240(3)–2.304(4) Å; cf. 2.19–2.30(2) Å in **9**). The C(3)–C(4) bond (1.436(5) Å) is somewhat longer than the other two C–C bonds in the ring (1.410–1.416(5) Å). The intra-ring angle at Ru(2) is 77.7(1)°, while angles at C within the ring are between 112.9 and 117.4(3)°.

Both C(3) and C(402) of the phenyl group attached to C(4) are metallated by Ru(3) (Ru(3)–C(3,402) 2.107(4), 2.128(4) Å). Coordination around this atom is completed by three CO groups and P(2) of the dppm ligand (Ru(3)–P(2) 2.383(2) Å). The other end of the dppm ligand is attached to Ru(1) (Ru(1)–P(1) 2.329(1) Å). Bond distances and angles in the dppm ligand are similar to those of other complexes. Coordination about Ru(3) is considerably distorted from ideal octahedral, with angle C(3)–Ru(3)–C(402) within the five-membered ring being 77.5(1)° (similar to that at Ru(2) above), and those subtended by C(3,33), C(33,402) and P(2), C(402) all being less than 90° (80.3–85.4(2)°).

2.2.3. *Molecular structure of* $Ru_3(\mu_3\text{-}C_4H_2Ph_2)(\mu\text{-}CO)(CO)_5(dppm)$ (**5**)

A molecule of **5** is shown in Fig. 3, and selected bond parameters are given in Table 3. The three ruthenium atoms form an open array which is spanned by the four atoms of a butadiendiyl ligand formed by partial hydrogenation of the original diyne. The geometry of the Ru_3C_4 unit is pentagonal bipyramidal. One of the Ru–Ru bonds carries a μ-CO ligand, while the unchanged dppm ligand now chelates the third ruthenium atom. Five terminal CO groups complete the coordination. The structure is related to that of the black isomer of $Fe_3(\mu\text{-}C_4R_4)(CO)_8$ [13,14], and the recently reported orange-yellow ruthenium analogue $Ru_3(\mu_3\text{-}C_4Ph_4)(\mu\text{-}CO)_2(CO)_6$ (**10**) [15].

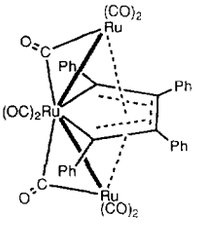

(10)

The bent Ru_3 chain (Ru(1,3)–Ru(2) 2.696(1), 2.669(1) Å; cf. 2.6696, 2.6717(8) Å in **10**) is attached to the $C_4H_2Ph_2$ unit by σ bonds to Ru(2) (Ru(2)–C(1,4) 2.225(6), 2.175(8) Å; cf. 2.219, 2.216(4) Å in **10**) and π-type bonds to Ru(1) and Ru(3) (range 2.295–2.366(8) Å; 2.283–2.356(4) Å in **10**). The angle at Ru(2) within the five-membered ring is 74.7(3)°, comparable with that found in **10** (74.1(2)°). Atoms Ru(2)C(1–4) are coplanar (χ^2 1.8; deviation of Ru(2) from C_4 plane 0.00(1) Å) and are normal to the Ru_3 plane (dihedral 89.7(2)°). Any trans effect on the butadienyl–metal bonds resulting from the presence of the dppm ligand is reflected in shorter Ru(1)–C(1,2) bonds, although this effect is carried over only to the Ru(3)–C(1) vector on the opposite side of the ring.

Ligand CO(33) symmetrically bridges the Ru(2)–Ru(3) vector (Ru(2,3)–C(33) 2.047, 2.042(7) Å), which

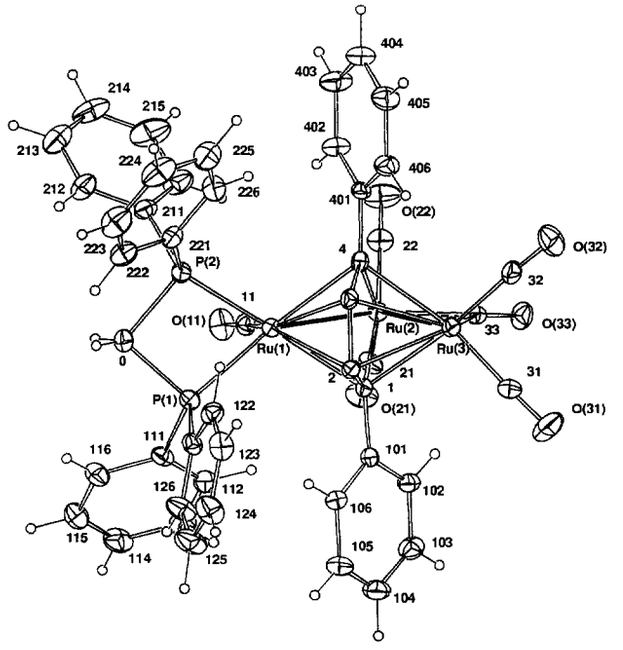

Fig. 3. Plot of a molecule of $Ru_3\{\mu_3\text{-}C_4H_2Ph_2\}(\mu\text{-}CO)(CO)_5(dppm)$ (**5**), showing the atom numbering scheme.

is shorter than the non-bridged Ru(1)–Ru(2) vector. The geometry of the dppm ligand is normal (Ru(1)–P(1,2) 2.299, 2.302(2); P(1)–Ru(1)–P(2) 71.36(9)°).

2.2.4. $Ru_2\{\mu\text{-}2\eta^1,\eta^4,\mu\text{-}2\eta^1PhCCCCPh[Ru_2(CO)_8]\}(CO)_6$ (7)

A molecule of **7** is shown in Fig. 4, and selected structural data are included in Table 4. As can be seen, there are two Ru_2 fragments which are linked by the diyne. In the first, the four-carbon unit interacts with one Ru atom via an η^4 mode and with the other by σ bonds to the extreme carbon atoms. The system is similar to the metallacyclopentadiene found in $Ru_2\{\mu\text{-}PhCC(C{\equiv}CPh)CPhC(C{\equiv}CPh)\}(CO)_6$ obtained from the earlier reaction [1] and in **4** above. However, **7** is derived from only one molecule of the diyne. The central two carbon atoms are σ bonded to and bridging an $Ru_2(CO)_8$ moiety, similar to that found in $Os_2\{\mu\text{-}C_2(CO_2Me)_2\}(CO)_8$ (**11**) [16]. An alternative description of the ring system is as a diruthenabicyclo[3.2.0]heptadiene.

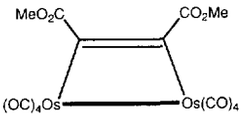

(11)

The Ru(1)–Ru(2) separation is 2.693(4) Å, considerably shorter than those found previously in similar complexes, but similar to that found for **9** (2.703(3) Å). This bond is semi-bridged by CO(21) as found in most previous structurally characterised examples [17,18]. The two $Ru(CO)_3$ groups are staggered when viewed down the Ru(1)–Ru(2) vector.

The organic ligand is attached to Ru(1) by two Ru–C σ bonds (Ru(1)–C(1,4) 2.08, 2.10(2) Å) and to Ru(2) in

Table 3
Selected bond parameters for $Ru_3\{\mu_3\text{-}C_4H_2Ph_2\}(\mu\text{-}CO)(CO)_5(dppm)$ (**5**)

Bond lengths (Å)		Bond angles (deg)	
Ru(1)–Ru(2)	2.696(1)	Ru(1)–Ru(2)–Ru(3)	89.43(3)
Ru(2)–Ru(3)	2.669(1)	P(1)–Ru(1)–P(2)	71.36(9)
Ru(1)–P(1)	2.299(2)	P(1)–C(0)–P(2)	93.9(4)
Ru(1)–P(2)	2.303(2)	C(1)–Ru(2)–C(4)	74.7(3)
Ru(1)–C(1)	2.296(7)		
Ru(1)–C(2)	2.295(7)	Ru(1)–P(1)–C(0)	96.3(3)
Ru(1)–C(3)	2.322(8)	Ru(1)–P(2)–C(0)	95.7(3)
Ru(1)–C(4)	2.322(8)		
Ru(2)–C(1)	2.225(6)	Ru(2)–C(1)–C(2)	117.9(5)
Ru(2)–C(4)	2.175(8)	C(1)–C(2)–C(3)	114.5(5)
Ru(3)–C(1)	2.296(8)	C(2)–C(3)–C(4)	114.2(7)
Ru(3)–C(2)	2.352(7)	Ru(2)–C(4)–C(3)	118.6(5)
Ru(3)–C(3)	2.366(7)		
Ru(3)–C(4)	2.355(6)		
Ru(2)–C(33)	2.047(8)		
Ru(3)–C(33)	2.042(7)		
P(1)–C(0)	1.828(8)		
P(2)–C(0)	1.845(9)		
C(1)–C(2)	1.43(1)		
C(2)–C(3)	1.48(1)		
C(3)–C(4)	1.454(8)		

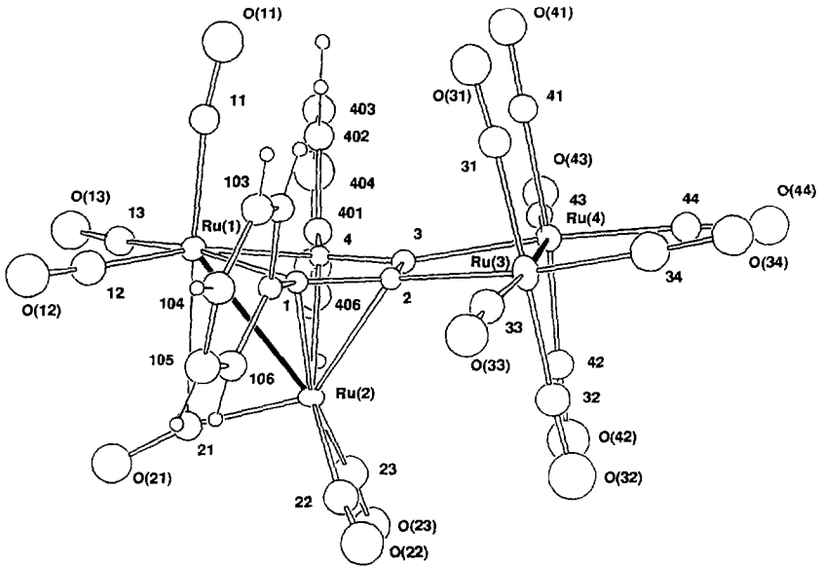

Fig. 4. Plot of a molecule of $Ru_2\{\mu\text{-}2\eta^1,\eta^4,\mu\text{-}2\eta^1\text{-}PhCCCCPh[Ru_2(CO)_8]\}$ (7), showing the atom numbering scheme.

the η^4 mode. As found previously, the outer carbons of the C_4 array are closer to Ru(2) than the inner carbons (Ru(2)–C(1,4) 2.24, 2.25(2) Å; Ru(2)–C(3,4) 2.35, 2.25(2) Å). Atoms C(1) and C(4) are each substituted by a phenyl group. Although the e.s.d.s are too large for meaningful comparisons, the C–C bonds within the C_4 array show the previously observed short–long–short alternation. Within the RuC_4 ring, angles at carbon range between 113–118(2)°.

Atoms Ru(3) and Ru(4) are separated by 2.874(3) Å. Although no other examples of $Ru_2(CO)_8$ groups attached to a bridging C_2 unit have been structurally characterised, in the related osmium complex **11** the Os–Os separation is 2.8975(1) [16]. Other related molecules are $Os_2(\mu\text{-}CH_2CHR)(CO)_8$, with Os–Os separations of 2.883(1) (R = H) [19] and 2.8850(5) Å ($R = CO_2Me$) [20], and $Ru_2(\mu\text{-}dppm)_2\{\mu\text{-}CH(CO_2Me)CH(CO_2Me)\}(CO)_4$, where the Ru–Ru separation has lengthened to 2.920(2) Å, probably because of the steric constraints exercised by the μ-dppm ligands [21]. In simple derivatives, Ru–Ru and Os–Os separations are usually comparable. Looking down the Ru(3)–Ru(4) vector, the two $Ru(CO)_4$ groups are seen to be eclipsed, as found in the related Os complex **11** [16]. The Ru–C σ bonds are within the normal range (2.13, 2.12(2)Å; cf. 2.138(5) Å in **11**) and angles at carbon are 109, 110(1)° (cf. 112.2(2)° in **11**). The reduction from the expected 120° is undoubtedly due to the strain imposed by bonding to the Ru_2 system. This is also demonstrated by the angles at Ru within the

Table 4
Selected structural parameters for $Ru_2\{\mu\text{-}2\eta^1,\eta^4,\mu\text{-}2\eta^1\text{-}PhCCCCPh[Ru_2(CO)_8]\}(CO)_6$ (7)

Bond lengths (Å)		Bond angles (deg)	
Ru(1)–Ru(2)	2.693(4)	C(1)–Ru(1)–C(4)	75.7(9)
Ru(3)–Ru(4)	2.874(3)	Ru(4)–Ru(3)–C(2)	70.6(6)
Ru(1)–C(1)	2.08(2)	Ru(3)–Ru(4)–C(3)	70.8(6)
Ru(1)–C(4)	2.10(2)	Ru(1)–C(1)–C(2)	118(2)
Ru(2)–C(1)	2.24(2)	C(1)–C(2)–C(3)	114(2)
Ru(2)–C(2)	2.31(2)	C(2)–C(3)–C(4)	113(2)
Ru(2)–C(3)	2.35(2)	C(3)–C(4)–Ru(1)	118(2)
Ru(2)–C(4)	2.25(2)	Ru(2)–C(2)–C(3)	73(1)
Ru(3)–C(2)	2.13(2)	Ru(4)–C(3)–C(2)	110(2)
Ru(4)–C(3)	2.12(2)	Ru(2)–C(21)–O(21)	167(2)
Ru(1)–C(21)	2.55(3)	Ru(1)–C(21)–O(21)	119(2)
Ru(2)–C(21)	1.81(3)		
C(1)–C(2)	1.39(3)		
C(2)–C(3)	1.47(3)		
C(3)–C(4)	1.37(3)		

four-membered ring, which are 70.6, 70.8(6)°, compared with 68.3(2)° in **11**. The C(2)–C(3) distance is 1.47(3) Å.

2.2.5. Comparison of dppm ligands

The three complexes **1**, **4** and **5** each contain a dppm ligand with different coordination geometries. In **1**, the dppm bridges two bonded ruthenium atoms, whereas in **4** the two Ru atoms are separate. In **5**, the dppm chelates a single Ru atom. Comparisons of various geometrical parameters shows that, in the chelate, the Ru–P distances (av. 2.301 Å) are about 0.05 Å shorter than those found for the bridging ligands (av. 2.350 Å for **1**, 2.356 Å for **4**). There appears to be no significant difference in the P–C(0) distances. Not surprisingly, average values for angles at P and C(0) within the chelate ring (96.0° and 93.9° respectively) are smallest in the chelate ring, increasing to 110.6°, 107.9° in the five-membered ring to 117.6°, 124.0° in **3**. The differences in the Ph–P–Ph (average values 100.7, 102.3 and 103.0°; range 100.3–105.6°) and C(0)–P–Ph angles (average values 103.8, 101.9 and 106.8°; range 98.9–108.1°) do not exceed the differences in individual bond angles. In the chelate **5**, the average Ru–P–Ph angle (121.3°) is significantly larger than the corresponding angles for **1** and **4** (117.9, 115.4°), possibly because of steric hindrance between the Ph groups and other ligands present.

3. Discussion

The reaction between $Ru_3(\mu\text{-dppm})(CO)_{10}$ and PhC≡CC≡CPh affords two complexes. The molecular structure of the major product, **1**, has been confirmed as being a conventional cluster-bound alkyne bearing a PhC≡C– substituent. Complex **2** is formed by coupling of two alkyne molecules and could be obtained in higher yield by further reaction of **1** with the diyne. It may have a structure related to those of similar complexes, such as $Ru_3(\mu_3\text{-}C_4(CO_2Me)_4)(\mu\text{-dppm})(CO)_6$ [9], with a C≡C triple bond taking the place of the coordinated ester CO group. Unfortunately, we have not been able to confirm this proposal by an X-ray study.

When **1** is heated in refluxing xylene for a short time, several alteration products are obtained, of which it has been possible to characterise the major product (as **4**) and one minor product (**5**) by X-ray studies. Complex **4** is an isomer of **1**, formed by metallation of one of the two phenyl groups of the original diyne, the H atom being located on atom C(2). The resulting ligand has an unusual 6:5:5 tricyclic ring system, in which two Ru atoms occupy opposing positions in the two five-membered rings. Unusually for thermolytic reactions of Ru_3–dppm clusters, the dppm ligand remains unchanged and is found bridging Ru(3) (which has been extruded from the original cluster) and one of the Ru atoms of the remaining Ru_2 fragment. In turn, this is found in the familiar Ru_2C_4 system, previously exemplified by the complexes $Ru_2(\mu\text{-}C_4R_2R'_2)(CO)_6$ (R = R′ = CO_2Me [17], CH_2OH [18]; 1,4 – R_2 = $(C_2H_4OH)_2$, 2,3 – R'_2 = Et_2 [18]; 1,4-R_2 = Fc, 2,3-R'_2 = H_2 (Fc = ferrocenyl) [12]; 1,3-R_2 = Ph_2, 2,4-R'_2 = $(C{\equiv}CPh)_2$ [1]).

The minor product **5** is found to be related to thermodynamic isomers of complexes $M_3(\mu_4\text{-}C_4Ph_4)(CO)_8$ (M = Fe, Ru, Os) [13–15,22], although differing in detail because of the presence of the dppm ligand chelating one of the Ru atoms. In particular, only one of the Ru–Ru vectors is bridged by CO, in contrast with the situation found with the parent complexes, in which both M–M bonds carry bridging CO ligands.

This study has revealed an additional facet of the behaviour of cluster coordinated 1,3-diynes. Conceptually, the simpler reaction is partial hydrogenation to a buta-1,3-diene (the additional H atoms presumably coming from the solvent) which is found bridging an open Ru_3 array. Alternatively, intramolecular metallation occurs with fragmentation of the cluster and formation of **5**. Again, the original C_4 system is able to pick up the H atom liberated by metallation of the Ph group; with the σ-bond to Ru(3) also present, the original C_4 chain is transformed into a buta-1,3-diene, this time found attached to the Ru_2L_6 system in conventional manner.

Comparison of the thermal alteration of **1** and **3** shows that complexes obtained from the former retain the Ru_3 core, whereas fragmentation occurs during thermolysis of the latter (Scheme 2). The products are formed either by combination of two Ru_2 fragments to give an Ru_4 core attached to one of the triple bonds, or by attachment of a second Ru_2 fragment to the ring carbon substituents of a ruthenacyclopentadiene complex.

The small amounts of **7** obtained precluded any study of the mechanism of formation. However, it is interesting that this reaction represents the first occasion on which a 1,3-diyne has been converted to a dimetallated 1,3-diene which is now able to chelate one of the metal atoms by virtue of the resulting rehybridisation of the carbons in the C_4 array. The bending away of the uncomplexed C≡CPh groups from the cluster in **3** suggests that intermolecular reactions are occurring. Perhaps these involve further coordination of the free C≡C triple bond to a ruthenium carbonyl fragment, followed by cluster fragmentation and rearrangement of the resulting intermediate to form the bis-binuclear system found in **7**.

4. Conclusion

While the reaction between $Ru_3(\mu\text{-dppm})(CO)_{10}$ and PhC≡CC≡CPh produced no surprises, in that the prod-

ucts include a conventional μ_3-alkyne complex and a coupling product with a second molecule of alkyne (diyne), the thermolysis of **1** has given two complexes in which the dppm ligand has remained unchanged, in spite of being heated at 130 °C. This is unusual, as on many previous occasions metallation and dephenylation reactions have been described under much milder conditions [23]. In the present case, however, it is the diyne which has altered, picking up H atoms, either from a phenyl substituent, or from solvent (presumably) to give ligands which can adopt familiar yet novel coordination modes. In neither case (**3** or **4**) are we able to comment on possible reaction mechanisms.

5. Experimental

5.1. Instrumentation

IR: Perkin–Elmer 1700X FT IR. NMR: Bruker CXP300 or ACP300 (^{1}H NMR at 300.13 MHz, ^{13}C NMR at 75.47 MHz). FAB MS: VG ZAB 2HF (using 3-nitrobenzyl alcohol as matrix, exciting gas Ar, FAB gun voltage 7.5 kV, current 1 mA, accelerating potential 7 kV).

5.2. General reaction conditions

Reactions were carried out under an atmosphere of nitrogen, but no special precautions were taken to exclude oxygen during work-up.

5.3. Starting materials

$Ru_3(CO)_{12}$ [24], $Ru_3(\mu\text{-dppm})(CO)_{10}$ [25] and PhC≡CC≡CPh [26] were prepared by literature methods. $Ru_3(\mu_3\text{-}PhC_2C{\equiv}CPh)(\mu\text{-}CO)(CO)_9$ was prepared as described earlier [1].

5.4. Preparation of $Ru_3(\mu_3\text{-}PhC_2C{\equiv}CPh)(\mu\text{-}dppm)(\mu\text{-}CO)(CO)_7$ (1)

5.4.1. From $Ru_3(\mu\text{-}dppm)(CO)_{10}$ and PhC≡CC≡CPh

Me_3NO (20 mg, 0.2 mmol) was added to a solution of $Ru_3(\mu\text{-dppm})(CO)_{10}$ (200 mg, 0.2 mmol) and PhC≡CC≡CPh (40 mg, 0.2 mmol) in thf (20 ml) and the mixture was stirred overnight at room temperature. Removal of solvent and separation of products by preparative t.l.c. (acetone–hexane 3:7) of a CH_2Cl_2 solution of the residue gave three coloured bands and a dark baseline. Band 1 (R_f 0.39) contained $Ru_3(\mu\text{-dppm})(CO)_{10}$ (84 mg, 42%). Band 2 (R_f 0.36) contained $Ru_3(\mu_3\text{-}PhC_2C{\equiv}CPh)(\mu\text{-dppm})(\mu\text{-}CO)(CO)_7$ (**1**), isolated as dark red crystals (80 mg, 36%) from CH_2Cl_2–hexane. Anal. Found: C, 52.48; H, 2.95. $C_{49}H_{32}O_8P_2Ru_3$. Calc.: C, 52.83; H, 2.88%. IR (cyclohexane): ν(CO) 2064vs, 2036m, 2029m, 2011s, 2002s, 1983(sh), 1976m(br), 1942w(br), 1855(sh), 1844m(br) cm^{-1}. ^{1}H NMR ($CDCl_3$): δ 4.49 (m, 1H, CH_2), 5.81 (m, 1H, CH_2), 6.92–7.51 (m, 30H, Ph). FAB mass spectrum (m/z): 1115, M^+; 1087–891, $[M - nCO]^+$ (n = 1–8); 813, $[M - 8CO - Ph]^+$; 735, $[M - 8CO - 2Ph]^+$. Band 3 (R_f 0.25) gave $Ru_3(\mu\text{-dppm})\{\mu\text{-}C_4Ph_2(C{\equiv}CPh)_2\}(CO)_6$ (**2**) (19 mg, 7%) as a dark purple powder. Anal. Found: C, 59.72; H, 3.90. Calc.: $C_{63}H_{42}O_6P_2Ru_3$. C, 60.05; H, 3.34%. IR (cyclohexane): ν(CO) 2027m, 2004vs, 1974m, 1967(sh), 1955m cm^{-1}. ^{1}H NMR ($CDCl_3$): δ 3.62 (m, 1H, CH_2), 4.83 (m, 1H, CH_2), 6.60–8.20 (m, 40H, Ph). FAB mass spectrum (m/z); 1261, M^+; 1233–1093, $[M - nCO]^+$ (n = 1–6); 1015, $[M - 6CO - Ph]^+$; 937, $[M - 6CO - 2Ph]^+$.

5.4.2. From $Ru_3(\mu_3\text{-}PhC_2C{\equiv}CPh)(\mu\text{-}CO)(CO)_9$ and dppm

A mixture of $Ru_3(\mu_3\text{-}PhC_2C{\equiv}CPh)(\mu\text{-}CO)(CO)_9$ (109 mg, 0.13 mmol) and dppm (51 mg, 0.13 mmol) was heated in refluxing thf (20 ml) for 10 min. Removal of solvent followed by preparative t.l.c. afforded $Ru_3(\mu_3\text{-}PhC_2C{\equiv}CPh)(\mu\text{-dppm})(\mu\text{-}CO)(CO)_7$ (**1**) (96 mg, 66%), identical with the product prepared in Section 5.4.1 above.

5.4.3. Reaction of $Ru_3(\mu_3\text{-}PhC_2C{\equiv}CPh)(\mu\text{-dppm})(\mu\text{-}CO)(CO)_7$ (1) with PhC≡CC≡CPh

Me_3NO (3 mg, 0.03 mmol) was added to a mixture of $Ru_3(\mu_3\text{-}PhC_2C{\equiv}CPh)(\mu\text{-dppm})(\mu\text{-}CO)(CO)_7$ (**1**) (25 mg, 0.02 mmol) and PhC≡CC≡CPh (7 mg, 0.03 mmol) was dissolved in thf (10 ml). After 30 min, the reaction was complete and t.l.c. separation afforded $Ru_3(\mu\text{-dppm})\{\mu\text{-}C_4Ph_2(C{\equiv}CPh)_2\}(CO)_6$ (**2**) (14 mg, 50%).

A similar reaction carried out in the absence of Me_3NO is complete in 10 h at room temperature or in a few minutes at reflux point.

5.5. Thermolysis of $Ru_3(\mu_3\text{-}PhC_2C{\equiv}CPh)(\mu\text{-dppm})(\mu\text{-}CO)(CO)_7$ (1)

A solution of $Ru_3(\mu_3\text{-}PhC_2C{\equiv}CPh)(\mu\text{-dppm})(\mu\text{-}CO)(CO)_7$ (**1**) (58 mg, 0.05 mmol) in xylene (7 ml) was heated in an oil-bath (130 °C) under nitrogen. After 30 min the colour of the solution had changed from purple to brown and t.l.c. showed that **1** was no longer present. After removal of solvent, a CH_2Cl_2 extract of the residue was separated by preparative t.l.c. (acetone–hexane 1:3) to give four bands. Band 1 (R_f 0.46, bright yellow) afforded yellow crystals of $Ru_3\{\mu_3\text{-}CPhCHCC(C_6H_4\text{-}2)\}(\mu\text{-dppm})(CO)_8$ (**4**) (36 mg, 61%) from CH_2Cl_2–MeOH. Anal. Found: C, 53.03; H, 2.94. $C_{49}H_{32}O_8P_2Ru_3$. Calc.: C, 52.83; H, 2.88%. IR (CH_2Cl_2): ν(CO) 2088s, 2048vs, 2022m, 2007m, 1983s, 1962w, 1923w cm^{-1}. ^{1}H NMR ($CDCl_3$): δ 1.37 (m, 2H, CH_2 + CH), 2.23 (q, J(HH) = 13 Hz,

J(HP) = 13 Hz, 1H, CH_2), 6.68–7.76 (3 × m, 29H, $PhCC_6H_4$). FAB mass spectrum (m/z): 1115, M^+; 1087–891, $[M - nCO]^+$ (n = 1–8); 814, $[M - 8CO - Ph]^+$; 737, $[M - 8CO - 2Ph]^+$. Band 3 (R_f 0.39, orange) gave red crystals (from C_6H_6–hexane) of $Ru_3\{\mu_3\text{-}C_4H_2Ph_2\}(\mu\text{-}CO)(CO)_5(dppm)$ (**5**) (4.7 mg, 9%). IR (CH_2Cl_2): ν(CO) 2019s, 1990vs, 1945m, 1808w(br) cm^{-1}. ^1H NMR ($CDCl_3$): δ 0.91 (m, 2H, CHCH), 4.21 (dt, J(HP) = 10 Hz, 1H, CH_2), 4.95 (dt, J(HP) = 10 z, 1H, CH_2), 6.50–7.49 (m, 30H, Ph). FAB mass spectrum (m/z): 1061, M^+; 977, $[M - 3CO]^+$; 948, $[M - 4CO]^+$; 820, $[M - 5CO - Ru]^-$; 791, $[M - 6CO - Ru]^+$. The other bands contained material which decomposed on attempted isolation and have not been identified.

5.6. Thermolysis of $Ru_3(\mu_3\text{-}PhC_2C{\equiv}CPh)(\mu\text{-}CO)(CO)_9$ (3)

A solution of $Ru_3(\mu_3\text{-}PhC_2C{\equiv}CPh)(\mu\text{-}CO)(CO)_9$ (87 mg, 0.111 mmol) in xylene (10 ml) was heated in an oil-bath (120 °C) for 30 min. After cooling to room temperature, solvent was removed in vacuo and the reaction products were separated by preparative t.l.c. (silica gel, acetone–hexane 3:7). The first yellow band (R_f 0.80) afforded $Ru_3(CO)_{12}$ (1 mg, 1.4%), identified from its infrared ν(CO) spectrum. A red band (R_f 0.65) gave $Ru_4(\mu_4\text{-}PhC_2C{\equiv}CPh)(CO)_{12}$ (**6**) (11 mg, 14%) as dark red crystals from hexane, identified by comparison with an authentic sample [1].

A second yellow band (R_f 0.57) gave yellow crystals of $Ru_2\{\mu\text{-}2\eta^1,\eta^4,\mu\text{-}2\eta^1\text{-}PhCCCCPh[Ru_2(CO)_8]\}$ (**7**) (4 mg, 5%) from CH_2Cl_2–EtOH. Infrared (CH_2Cl_2): ν(CO) 2126w, 2089m, 2070m, 2048vs, 2023m, 2008m, 1985m(br), 1915m(br) cm^{-1}. FAB MS (m/z): 1000, M^+; 972–608, $[M - nCO]^+$ (n = 1–14). Several other complexes formed in this reaction (total yield 14 mg) were obtained in amounts too small to permit characterisation.

6. Crystallography

Unique data sets were measured at ca. 295 K within the specified $2\theta_{max}$ limits using an Enraf–Nonius CAD4 diffractometer (2θ–θ scan mode; monochromatic Mo Kα radiation, λ 0.7107$_3$ Å); N independent reflections were obtained, N_o with $I > 3\sigma(I)$ being considered 'observed' and used in the full matrix least squares refinement after Gaussian absorption correction. Anisotropic thermal parameters were refined for the non-hydrogen atoms; (x, y, z, U_{iso})$_H$ were included constrained at estimated values. Conventional residuals R, R' on $|F|$ are quoted, statistical weights derivative of $\sigma^2(I) = \sigma^2(I_{diff}) + 0.0004\sigma^4(I_{diff})$ being used. Computation used the XTAL 3.0 program system [27] implemented by Hall and Stewart; neutral atom complex scattering factors were employed. Pertinent results are given in the figures and Tables 1–9. Thermal and hydrogen parameters, and full molecular non-hydrogen geometries have been deposited at the Cambridge Crystallographic Data Centre.

Table 5
Crystal data and refinement details for complexes **1**, **4**, **5** and **7**

Compound	**1**	**4**	**5**	**7**
Formula	$C_{49}H_{32}O_8P_2Ru_3$	$C_{49}H_{32}O_8P_2Ru_3$	$C_{47}H_{32}O_6P_2Ru_3.C_6H_6$	$C_{30}H_{10}O_{14}Ru_4$
MW	1114.0	1114.0	1136.0	998.7
Crystal system	Monoclinic	Triclinic	Monoclinic	Orthorhombic
Space group	$P2_1/c$ (No. 14)	$P\bar{1}$ (No. 2)	$P2_1/c$ (No. 14)	$P2_12_12_1$ (No. 19)
a (Å)	12.722(4)	17.676(4)	13.804(7)	27.013(11)
b (Å)	30.893(11)	12.331(9)	22.148(9)	12.565(5)
c (Å)	12.397(3)	11.238(6)	16.565(7)	9.412(14)
α (deg)		69.52(7)		
β (deg)	112.12(3)	71.62(3)	112.38(4)	
γ (deg)		79.01(3)		
V (Å^3)	4513	2169	4683	3195
Z	4	2	4	4
D_c (g cm^{-3})	1.639	1.706	1.611	2.075
F(000)	2208	1104	2216	1912
μ (cm^{-1})	11.2	11.6	10.7	19.2
Crystal size (mm^3)	0.06 × 0.17 × 0.58	0.28 × 0.12 × 0.33	0.07 × 0.35 × 0.25	0.09 × 0.09 × 0.27
A^* (min, max)	1.07, 1.22	1.14, 1.35	1.08, 1.32	1.17, 1.19
$2\theta_{max}$ (deg)	50	60	50	50
N	7935	12608	8224	3169
N_o	5082	7666	4905	2049
R	0.039	0.037	0.045	0.067
R_w	0.038	0.032	0.042	0.069

Table 6
Non-hydrogen positional and isotropic displacement parameters, (1)

Atom	x	y	z	U_{eq} (Å^2)
Ru(1)	0.91261(4)	0.41750(2)	0.62741(4)	0.0301(2)
Ru(2)	0.81562(4)	0.35641(2)	0.72819(5)	0.0348(2)
Ru(3)	0.94663(5)	0.42827(2)	0.85519(5)	0.0371(2)
C(11)	1.0211(6)	0.4544(2)	0.6075(5)	0.040(3)
O(11)	1.0867(5)	0.4764(2)	0.5988(5)	0.067(3)
C(12)	0.8047(6)	0.4621(2)	0.5951(6)	0.045(3)
O(12)	0.7448(5)	0.4910(2)	0.5814(5)	0.068(3)
C(21)	0.8228(6)	0.2961(3)	0.7626(6)	0.049(3)
O(21)	0.8337(5)	0.2604(2)	0.7899(5)	0.082(3)
C(22)	0.6704(7)	0.3693(3)	0.7368(7)	0.063(4)
O(22)	0.5898(5)	0.3751(3)	0.7516(6)	0.116(4)
C(23)	0.8767(6)	0.3657(2)	0.9003(6)	0.048(3)
O(23)	0.8799(4)	0.3528(2)	0.9896(4)	0.065(3)
C(31)	1.0371(7)	0.4248(2)	1.0192(6)	0.054(4)
O(31)	1.0946(5)	0.4235(2)	1.1143(5)	0.087(3)
C(32)	1.0175(6)	0.4803(2)	0.8360(6)	0.049(3)
O(32)	1.0610(5)	0.5117(2)	0.8294(5)	0.075(3)
C(33)	0.8153(7)	0.4599(2)	0.8595(7)	0.057(4)
O(33)	0.7373(5)	0.4777(2)	0.8590(6)	0.091(3)
P(1)	0.8793(1)	0.38540(5)	0.4468(1)	0.0335(7)
C(111)	1.0035(5)	0.3698(2)	0.4153(5)	0.038(3)
C(112)	1.0343(6)	0.3280(2)	0.4071(6)	0.054(4)
C(113)	1.1327(8)	0.3191(3)	0.3880(8)	0.077(5)
C(114)	1.1986(7)	0.3519(3)	0.3746(7)	0.074(5)
C(115)	1.1674(7)	0.3942(3)	0.3796(7)	0.068(4)
C(116)	1.0690(6)	0.4035(2)	0.3983(6)	0.051(3)
C(121)	0.7920(5)	0.4114(2)	0.3099(5)	0.037(3)
C(122)	0.7789(6)	0.3928(2)	0.2043(6)	0.053(3)
C(123)	0.7141(7)	0.4125(3)	0.1018(6)	0.062(4)
C(124)	0.6617(6)	0.4509(3)	0.1019(6)	0.056(3)
C(125)	0.6710(6)	0.4698(2)	0.2049(7)	0.056(3)
C(126)	0.7371(6)	0.4500(2)	0.3089(6)	0.044(3)
C(0)	0.8077(5)	0.3345(2)	0.4453(5)	0.037(3)
P(2)	0.7169(1)	0.34186(6)	0.5283(2)	0.0360(7)
C(211)	0.6429(6)	0.2899(2)	0.5078(6)	0.047(3)
C(212)	0.5331(7)	0.2882(3)	0.5043(8)	0.069(4)
C(213)	0.4785(8)	0.2483(3)	0.4936(9)	0.089(5)
C(214)	0.532(1)	0.2113(4)	0.487(1)	0.106(7)
C(215)	0.639(1)	0.2125(3)	0.4908(9)	0.094(6)
C(216)	0.6947(7)	0.2520(3)	0.5015(8)	0.072(5)
C(221)	0.6020(5)	0.3767(2)	0.4375(6)	0.042(3)
C(222)	0.5660(6)	0.4122(2)	0.4818(7)	0.054(3)
C(223)	0.4760(7)	0.4371(3)	0.411(1)	0.085(5)
C(224)	0.4237(7)	0.4271(4)	0.298(1)	0.096(5)
C(225)	0.4580(8)	0.3916(3)	0.2518(8)	0.094(5)
C(226)	0.5464(7)	0.3668(2)	0.3208(7)	0.059(4)
C(1)	1.0725(6)	0.2878(2)	0.6704(6)	0.041(3)
C(101)	1.1359(6)	0.2542(2)	0.6429(6)	0.043(3)
C(102)	1.0844(6)	0.2237(2)	0.5607(7)	0.059(4)
C(103)	1.1462(8)	0.1923(3)	0.5295(8)	0.071(4)
C(104)	1.2611(9)	0.1927(3)	0.5827(9)	0.081(5)
C(105)	1.3153(7)	0.2223(3)	0.6675(9)	0.087(5)
C(106)	1.2526(7)	0.2539(3)	0.6972(7)	0.065(4)
C(2)	1.0297(5)	0.3196(2)	0.6909(5)	0.036(3)
C(3)	0.9821(5)	0.3565(2)	0.7270(5)	0.035(3)
C(4)	1.0466(5)	0.3907(2)	0.7899(5)	0.031(2)
C(401)	1.1704(5)	0.3962(2)	0.8133(5)	0.035(3)
C(402)	1.2156(5)	0.3846(2)	0.7304(6)	0.044(3)
C(403)	1.3280(6)	0.3897(2)	0.7528(6)	0.054(3)
C(404)	1.4015(6)	0.4065(3)	0.8559(7)	0.055(3)
C(405)	1.3588(6)	0.4195(2)	0.9362(6)	0.054(3)
C(406)	1.2442(6)	0.4142(2)	0.9153(6)	0.044(3)

Table 7
Non-hydrogen positional and isotropic displacement parameters, (**4**)

Atom	x	y	z	U_{eq} (Å^2)
Ru(1)	0.73830(2)	0.20483(3)	0.52421(3)	0.0314(1)
Ru(2)	0.75846(2)	0.43526(3)	0.45033(3)	0.0352(1)
Ru(3)	0.86998(2)	0.13217(3)	0.79396(3)	0.0353(1)
C(11)	0.6644(2)	0.2813(4)	0.4267(4)	0.045(2)
O(11)	0.6211(2)	0.3160(3)	0.3618(3)	0.065(2)
C(12)	0.7638(3)	0.0828(4)	0.4488(4)	0.053(2)
O(12)	0.7820(2)	0.0171(3)	0.3940(4)	0.089(2)
C(21)	0.8375(3)	0.5156(3)	0.4533(4)	0.048(2)
O(21)	0.8879(2)	0.5590(3)	0.4550(3)	0.076(2)
C(22)	0.7528(2)	0.5201(4)	0.2719(4)	0.048(2)
O(22)	0.7521(2)	0.5722(3)	0.1669(3)	0.076(2)
C(23)	0.6638(2)	0.5323(3)	0.5086(4)	0.049(2)
O(23)	0.6086(2)	0.5951(3)	0.5304(4)	0.078(2)
C(31)	0.8989(2)	0.0816(4)	0.9616(5)	0.048(2)
O(31)	0.9170(2)	0.0613(3)	1.0550(3)	0.072(2)
C(32)	0.9622(2)	0.0438(4)	0.7099(4)	0.050(2)
O(32)	1.0164(2)	−0.0027(3)	0.6579(4)	0.080(2)
C(33)	0.9235(2)	0.2710(4)	0.7303(4)	0.051(2)
O(33)	0.9515(2)	0.3565(3)	0.6912(3)	0.079(2)
P(1)	0.64417(5)	0.11036(8)	0.7135(1)	0.0330(4)
C(111)	0.5978(2)	−0.0011(3)	0.6953(4)	0.038(2)
C(112)	0.5176(3)	0.0092(5)	0.7010(6)	0.066(3)
C(113)	0.4856(3)	−0.0752(6)	0.6845(7)	0.094(4)
C(114)	0.5317(3)	−0.1723(5)	0.6629(6)	0.075(3)
C(115)	0.6106(3)	−0.1853(4)	0.6572(5)	0.056(2)
C(116)	0.6428(3)	−0.1005(4)	0.6732(5)	0.047(2)
C(121)	0.5574(2)	0.2010(3)	0.7797(4)	0.035(2)
C(122)	0.5318(3)	0.3046(4)	0.6972(5)	0.055(2)
C(123)	0.4682(3)	0.3771(5)	0.7459(6)	0.067(3)
C(124)	0.4301(3)	0.3460(5)	0.8776(6)	0.065(3)
C(125)	0.4534(3)	0.2445(5)	0.9607(5)	0.057(2)
C(126)	0.5157(2)	0.1721(4)	0.9117(5)	0.049(2)
C(0)	0.6763(2)	0.0342(3)	0.8652(4)	0.035(2)
P(2)	0.78090(6)	−0.01511(8)	0.8675(1)	0.0352(4)
C(211)	0.7701(2)	−0.0910(3)	1.0427(4)	0.035(2)
C(212)	0.7022(3)	−0.0821(4)	1.1430(4)	0.053(2)
C(213)	0.7016(3)	−0.1375(4)	1.2731(5)	0.061(2)
C(214)	0.7681(3)	−0.2003(4)	1.3060(5)	0.054(2)
C(215)	0.8357(3)	−0.2105(4)	1.2079(5)	0.055(2)
C(216)	0.8367(3)	−0.1590(4)	1.0779(5)	0.047(2)
C(221)	0.8054(2)	−0.1355(3)	0.7993(4)	0.038(2)
C(222)	0.7730(3)	−0.2407(4)	0.8745(5)	0.050(2)
C(223)	0.7881(3)	−0.3317(4)	0.8237(6)	0.068(3)
C(224)	0.8347(4)	−0.3186(5)	0.6971(7)	0.074(3)
C(225)	0.8659(3)	−0.2156(5)	0.6220(6)	0.066(3)
C(226)	0.8524(3)	−0.1235(4)	0.6721(5)	0.049(2)
C(1)	0.8418(2)	0.3074(3)	0.3908(4)	0.034(2)
C(101)	0.8865(2)	0.3189(3)	0.2506(4)	0.036(2)
C(102)	0.9681(3)	0.3291(4)	0.2115(5)	0.048(2)
C(103)	1.0109(3)	0.3507(4)	0.0809(5)	0.057(2)
C(104)	0.9740(3)	0.3585(4)	−0.0111(5)	0.056(2)
C(105)	0.8938(3)	0.3476(4)	0.0249(5)	0.056(2)
C(106)	0.8511(3)	0.3258(4)	0.1558(4)	0.047(2)
C(2)	0.8687(2)	0.2198(3)	0.4928(4)	0.034(2)
C(3)	0.8298(2)	0.2198(3)	0.6240(4)	0.033(1)
C(4)	0.7655(2)	0.3102(3)	0.6318(4)	0.032(1)
C(401)	0.7298(2)	0.3130(3)	0.7694(4)	0.034(2)
C(402)	0.7663(2)	0.2357(3)	0.8654(4)	0.036(2)
C(403)	0.7333(3)	0.2346(4)	0.9959(4)	0.048(2)
C(404)	0.6665(3)	0.3075(5)	1.0321(5)	0.059(2)
C(405)	0.6323(3)	0.3841(4)	0.9387(5)	0.058(2)
C(406)	0.6636(2)	0.3878(4)	0.8078(5)	0.048(2)

Table 8
Non-hydrogen positional and isotropic displacement parameters, (**5**)

Atom	x	y	z	U_{eq} (Å^2)
Ru(1)	0.94812(5)	0.21516(3)	0.73784(4)	0.0368(2)
Ru(2)	0.87995(5)	0.32587(3)	0.67352(4)	0.0392(2)
Ru(3)	0.92721(5)	0.36603(3)	0.83600(4)	0.0423(3)
C(11)	0.9185(6)	0.2137(3)	0.6189(5)	0.047(3)
O(11)	0.9055(5)	0.2053(3)	0.5471(3)	0.073(3)
C(21)	0.9382(6)	0.3463(3)	0.5920(5)	0.050(3)
O(21)	0.9772(4)	0.3547(3)	0.5426(4)	0.077(3)
C(22)	0.7483(6)	0.3308(4)	0.5848(5)	0.058(4)
O(22)	0.6661(5)	0.3342(3)	0.5300(4)	0.094(3)
C(31)	1.0229(6)	0.4231(4)	0.8983(5)	0.060(4)
O(31)	1.0807(5)	0.4603(3)	0.9343(4)	0.099(4)
C(32)	0.8415(7)	0.4033(4)	0.8842(6)	0.065(4)
O(32)	0.7915(6)	0.4275(3)	0.9147(5)	0.110(4)
C(33)	0.8731(5)	0.4109(3)	0.7195(5)	0.045(3)
O(33)	0.8557(4)	0.4605(2)	0.6940(3)	0.067(3)
P(1)	1.0829(2)	0.14833(9)	0.7584(1)	0.0438(9)
C(111)	1.1579(6)	0.1482(3)	0.6892(5)	0.048(3)
C(112)	1.1764(6)	0.2010(4)	0.6531(5)	0.056(4)
C(113)	1.2322(7)	0.1998(4)	0.5988(5)	0.067(4)
C(114)	1.2692(7)	0.1465(4)	0.5820(6)	0.076(5)
C(115)	1.2521(7)	0.0946(4)	0.6172(6)	0.075(5)
C(116)	1.1978(6)	0.0943(4)	0.6729(5)	0.063(4)
C(121)	1.1783(6)	0.1377(3)	0.8691(5)	0.046(3)
C(122)	1.1445(6)	0.1366(3)	0.9376(5)	0.053(4)
C(123)	1.2142(7)	0.1348(4)	1.0224(5)	0.067(4)
C(124)	1.3195(7)	0.1336(4)	1.0412(5)	0.079(5)
C(125)	1.3551(7)	0.1353(5)	0.9750(6)	0.089(5)
C(126)	1.2853(6)	0.1368(4)	0.8884(5)	0.072(4)
C(0)	1.0015(6)	0.0805(3)	0.7276(5)	0.051(4)
P(2)	0.8850(2)	0.11840(9)	0.7329(1)	0.0435(9)
C(211)	0.7741(6)	0.0909(4)	0.6395(5)	0.050(3)
C(212)	0.7534(7)	0.0301(4)	0.6299(5)	0.074(4)
C(213)	0.6701(8)	0.0084(4)	0.5612(6)	0.090(5)
C(214)	0.6038(7)	0.0467(5)	0.5014(6)	0.095(5)
C(215)	0.6231(8)	0.1055(5)	0.5085(6)	0.109(6)
C(216)	0.7083(7)	0.1283(4)	0.5770(6)	0.080(5)
C(221)	0.8570(6)	0.0849(3)	0.8207(5)	0.050(4)
C(222)	0.9058(7)	0.0341(4)	0.8660(5)	0.064(4)
C(223)	0.8759(8)	0.0081(4)	0.9289(6)	0.088(5)
C(224)	0.7940(8)	0.0339(5)	0.9454(6)	0.087(5)
C(225)	0.7462(8)	0.0846(4)	0.9031(6)	0.080(5)
C(226)	0.7769(7)	0.1106(4)	0.8403(5)	0.063(4)
C(101)	1.1350(5)	0.3245(3)	0.7929(5)	0.045(3)
C(102)	1.1530(6)	0.3754(3)	0.7502(5)	0.048(3)
C(103)	1.2535(6)	0.3903(4)	0.7576(5)	0.060(4)
C(104)	1.3379(6)	0.3565(4)	0.8068(6)	0.070(4)
C(105)	1.3224(6)	0.3077(4)	0.8513(6)	0.068(4)
C(106)	1.2220(6)	0.2917(3)	0.8444(5)	0.053(4)
C(1)	1.0285(5)	0.3064(3)	0.7859(4)	0.038(3)
C(2)	1.0219(5)	0.2751(3)	0.8589(4)	0.040(3)
C(3)	0.9137(5)	0.2604(3)	0.8505(4)	0.041(3)
C(4)	0.8330(5)	0.2791(3)	0.7683(4)	0.038(3)
C(401)	0.7232(5)	0.2670(3)	0.7626(5)	0.043(3)
C(402)	0.6443(6)	0.2493(4)	0.6866(5)	0.060(4)
C(403)	0.5446(6)	0.2362(5)	0.6815(6)	0.081(5)
C(404)	0.5201(6)	0.2395(4)	0.7554(6)	0.080(5)
C(405)	0.5962(7)	0.2566(4)	0.8312(6)	0.072(5)
C(406)	0.6982(6)	0.2710(4)	0.8363(5)	0.057(4)

Table 8 (continued)

Atom	x	y	z	U_{eq} (Å^2)
C(01)	0.594(1)	0.4366(7)	0.683(1)	0.18(1)
C(02)	0.5579(9)	0.4343(7)	0.743(1)	0.18(1)
C(03)	0.508(1)	0.4800(8)	0.7596(8)	0.174(9)
C(04)	0.500(1)	0.5278(6)	0.717(1)	0.18(1)
C(05)	0.529(1)	0.5335(8)	0.652(1)	0.21(1)
C(06)	0.580(1)	0.486(1)	0.628(1)	0.26(1)

Table 9
Non-hydrogen positional and isotropic displacement parameters, (7)

Atom	x	y	z	U_{eq} (Å^2)
Ru(1)	0.39758(9)	0.4188(2)	0.5578(2)	0.0321(7)
Ru(2)	0.39298(9)	0.3170(2)	0.3064(2)	0.0311(7)
Ru(3)	0.31480(9)	0.0630(2)	0.4521(3)	0.0444(9)
Ru(4)	0.41904(8)	0.0212(2)	0.4770(2)	0.0350(7)
C(11)	0.390(1)	0.382(2)	0.749(3)	0.044(7)
O(11)	0.3874(9)	0.347(2)	0.859(3)	0.082(8)
C(12)	0.358(1)	0.542(3)	0.564(4)	0.059(9)
O(12)	0.3312(9)	0.613(2)	0.574(3)	0.093(9)
C(13)	0.457(1)	0.493(2)	0.576(3)	0.043(8)
O(13)	0.4938(8)	0.541(2)	0.597(2)	0.074(7)
C(21)	0.404(1)	0.459(2)	0.293(3)	0.043(8)
O(21)	0.4118(8)	0.549(2)	0.255(2)	0.076(7)
C(22)	0.345(1)	0.308(3)	0.158(4)	0.06(1)
O(22)	0.3122(9)	0.296(2)	0.091(3)	0.090(8)
C(23)	0.440(1)	0.284(3)	0.172(4)	0.06(1)
O(23)	0.4698(8)	0.268(2)	0.082(3)	0.067(7)
C(31)	0.306(1)	0.072(3)	0.657(3)	0.050(9)
O(31)	0.3014(9)	0.084(2)	0.778(3)	0.081(8)
O(32)	0.330(1)	0.050(2)	0.132(3)	0.11(1)
C(32)	0.327(1)	0.056(3)	0.253(4)	0.057(9)
C(33)	0.252(1)	0.118(2)	0.425(4)	0.058(9)
O(33)	0.212(1)	0.150(2)	0.395(3)	0.092(9)
C(34)	0.297(1)	−0.077(3)	0.454(4)	0.08(1)
O(34)	0.2855(8)	−0.171(2)	0.459(3)	0.081(7)
C(41)	0.4077(9)	0.025(2)	0.679(3)	0.040(7)
O(41)	0.4042(7)	0.027(2)	0.804(2)	0.068(6)
C(42)	0.429(1)	0.034(2)	0.283(3)	0.044(8)
O(42)	0.4388(8)	0.037(2)	0.165(3)	0.088(8)
C(43)	0.4872(9)	0.021(2)	0.499(3)	0.033(7)
O(43)	0.5298(7)	0.011(2)	0.523(2)	0.059(6)
C(44)	0.412(1)	−0.134(2)	0.458(3)	0.044(8)
O(44)	0.4060(8)	−0.225(2)	0.439(2)	0.076(7)
C(1)	0.3417(8)	0.316(2)	0.493(2)	0.024(6)
C(101)	0.2884(9)	0.351(2)	0.502(3)	0.028(6)
C(102)	0.262(1)	0.328(2)	0.624(3)	0.042(8)
C(103)	0.212(1)	0.358(2)	0.638(3)	0.051(8)
C(104)	0.191(1)	0.418(2)	0.535(3)	0.052(8)
C(105)	0.218(1)	0.448(3)	0.416(4)	0.061(9)
C(106)	0.265(1)	0.412(2)	0.400(3)	0.047(8)
C(2)	0.3538(8)	0.210(2)	0.471(3)	0.024(6)
C(3)	0.4071(8)	0.188(2)	0.482(3)	0.028(6)
C(4)	0.4348(8)	0.277(2)	0.506(2)	0.022(6)
C(401)	0.4897(9)	0.269(2)	0.532(3)	0.039(7)
C(402)	0.504(1)	0.248(2)	0.672(3)	0.043(8)
C(403)	0.555(1)	0.238(2)	0.700(3)	0.051(8)
C(404)	0.589(1)	0.252(3)	0.604(4)	0.08(1)
C(405)	0.576(1)	0.273(3)	0.463(4)	0.07(1)
C(406)	0.526(1)	0.280(2)	0.431(3)	0.047(8)

6.1. Abnormal features and variations in procedure

(**4**). Hydrogen atoms were refined in $(x, y, z, U_{iso})_H$.

(**5**). Difference map artefacts were modelled as C_6H_6, site occupancy set at unity after trial refinement.

(**7**). Weak data from a small specimen in the context of a non-centrosymmetric space group would support meaningful anisotropic thermal parameter refinement for Ru only, C, O being refined with the isotropic form.

Acknowledgements

We thank the Australian Research Council for support of this work and Johnson Matthey Technology plc for a generous gift of $RuCl_3 \cdot nH_2O$. NNZ thanks the Director, INEOS, Moscow, for leave of absence during which this work was carried out.

References

[1] M.I. Bruce, N.N. Zaitseva, B.W. Skelton and A.H. White, *Inorg. Chim. Acta*, in press.

[2] (a) J.F. Corrigan, S. Doherty, N.J. Taylor and A.J. Carty, *Organometallics, 11* (1992) 3160; (b) J.F. Corrigan, N.J. Taylor and A.J. Carty, *Organometallics, 13* (1994) 3778; (c) P. Blenkiron, N.J. Taylor and A.J. Carty, *J. Chem. Soc. Chem. Commun.*, (1995) 327.

[3] A.J. Deeming, M.S.B. Felix and D. Nuel, *Inorg. Chim. Acta, 213* (1993) 3.

[4] T.-K. Huang, Y. Chi, S.-M. Peng, G.-H. Lee, S.-L. Wang and F.-L. Liao, *Organometallics, 14* (1995) 2164.

[5] M.I. Bruce, N.N. Zaitseva, B.W. Skelton and A.H. White, *Polyhedron, 14* (1995) 2647.

[6] M.I. Bruce, N.N. Zaitseva, B.W. Skelton and A.H. White, *J. Cluster Sci., 7* (1996) 109.

[7] M.I. Bruce, P.J. Low, B.W. Skelton, A. Werth and A.H. White, *J. Chem. Soc. Dalton Trans.*, (1996) 1551.

[8] S. Rivomanana, G. Lavigne, N. Lugan and J.-J. Bonnet, *Inorg. Chem., 30* (1991) 4110.

[9] M.I. Bruce, P.A., Humphrey, H. Miyamae, B.W. Skelton and A.H. White, *J. Organomet. Chem., 429* (1992) 187.

[10] M.I. Bruce, B.W. Skelton, A.H. White and N.N. Zaitseva, *Aust. J. Chem., 49* (1996) 155.

[11] A.W. Coleman, D.F. Jones, P.H. Dixneuf, C. Brisson, J.-J. Bonnet and G. Lavigne, *Inorg. Chem., 23* (1984) 952.

[12] A.A. Koridze, A.I. Yanovsky and Yu.T. Struchkov, *J. Organomet. Chem., 441* (1992) 277.

[13] W. Hübel and E.H. Braye, *J. Inorg. Nucl. Chem., 10* (1959) 250.

[14] R.P. Dodge and V. Schomaker, *J. Organomet. Chem., 3* (1965) 274.

[15] M.V. Capparelli, Y. de Sanctis and A.J. Arce, *Acta Crystallogr. Sect. C:, 51* (1995) 1819.

[16] M.R. Burke and J. Takats, *J. Organomet. Chem., 302* (1986) C25.

[17] M.I. Bruce, J.G. Matisons, B.W. Skelton and A.H. White, *J. Organomet. Chem., 251* (1983) 249.

[18] A. Astier, J.-C. Daran, Y. Jeannin and C. Rigault, *J. Organomet. Chem., 241* (1983) 53.

[19] (a) K.M. Motyl, J.R. Norton, C.K. Schauer and O.P. Anderson, *J. Am. Chem. Soc., 104* (1982) 7325; (b) O.P. Anderson, B.R. Bender, J.R. Norton, A.C. Larson and P.J. Vergamini, *Organometallics, 10* (1991) 3145.

[20] M.R. Burke, J. Takats, F.-W. Grevels and J.G.A. Reuvers, *J. Am. Chem. Soc., 105* (1983) 4092.

[21] K.A. Johnson and W.A. Gladfelter, *Organometallics, 10* (1991) 377.

[22] G. Ferraris and G. Gervasio, *J. Chem. Soc. Dalton Trans.*, (1974) 1813.

[23] N. Lugan, J.-J. Bonnet and J.A. Ibers, *J. Am. Chem. Soc., 107* (1988) 4484.

[24] M.I. Bruce, C.M. Jensen and N.L. Jones, *Inorg. Synth., 26* (1989) 259; *28* (1990) 216.

[25] M.I. Bruce, B.K. Nicholson and M.L. Williams, *Inorg. Synth., 26* (1989) 276; *28* (1990) 225.

[26] I.D. Campbell and G. Eglinton, *Org. Synth. Coll., 5* (1973) 517.

[27] S.R. Hall and J.M. Stewart (eds.), XTAL *Users' Manual*, Version 3.0, 1990, Universities of Western Australia and Maryland.